Defect evolution of low energy, amorphizing germanium implants in silicon

A. C. King,[a] A. F. Gutierrez, A. F. Saavedra, and K. S. Jones
Department of Materials Science and Engineering, University of Florida, Gainesville, Florida 32611

D. F. Downey
Varian Semiconductor Equipment Associates, Gloucester, Massachusetts 01930

(Received 16 October 2002; accepted 8 December 2002)

The defect evolution upon annealing of low energy, amorphizing germanium implants into silicon was studied using plan-view transmission electron microscopy. Implants with energies of 5–30 keV at an amorphizing dose of 1×10^{15} Ge^+ cm^{-2} were annealed at 750 °C from 10 s to 360 min. For the implant energies of 10 and 30 keV, the defects form clusters which evolve to {311} defects that subsequently dissolve or form stable dislocation loops. However, as implant energy drops to 5 keV, the interstitials evolve from clusters to small, unstable loops which dissolve within a small time window and do not form {311}'s. To determine the effect of the free surface as an interstitial recombination sink for 5 keV implants, the amorphous layer of a 10 keV implant was lapped to less than the thickness of a 5 keV amorphous layer and then annealed. We found that the defect dissolution observed for the 5 keV implant energy was dependent on the implant energy and not the proximity of the end-of-range damage to the surface. The activation energy of the observed rapid defect dissolution at 5 keV was calculated to be 1.0 ± 0.1 eV. © *2003 American Institute of Physics.* [DOI: 10.1063/1.1542936]

I. INTRODUCTION

Preamorphization is a common technique used in the formation of ultrashallow junctions for Si-based microelectronics.[1–3] This step introduces end-of-range (EOR) defects below the amorphous/crystalline interface, which influence dopant diffusion and activation.[4] The excess interstitials in the EOR region are a source for transient enhanced diffusion (TED).[5] The behavior of the excess interstitials is especially important in understanding the formation of ultrashallow junctions at the low energy regime (<5 keV).

Nonamorphizing Si^+ implants have been previously studied,[6–9] and a consensus regarding the effect of interstitial evolution on TED has emerged.[10] In essence, the path includes the formation of small precursor clusters, which coalesce into {311} defects, which then either dissolve or transform into dislocation loops.[7,9] At longer times, these loops either dissolve and drive TED, or become stable and trap interstitials. Recently there has been interest in using low energy Ge^+ implants to preamorphize the Si surface prior to dopant implantation.[11] For reasons not understood, a 5 keV implant appears to result in the least amount of diffusion. The objective of this work is to characterize the defect evolution for low energy amorphizing implants.

II. EXPERIMENT

Czochralski grown (100) Si wafers were implanted at room temperature with a constant dose of 1×10^{15} Ge^+ cm^{-2} at 5, 10, and 30 keV energies with a 7° tilt. Cross-section transmission electron microscopy (XTEM) was used to measure the amorphous layer thickness produced from the implants. A JEOL 2010 high-resolution TEM operating at energy of 200 keV measured the amorphous layer thickness for the 5 and 10 keV energies to be 100 and 180 Å, respectively. The 30 keV energy amorphous layer thickness was measured to 480 Å by a JEOL 200 CX TEM.

Plan-view TEM (PTEM) specimens were first annealed at 750 °C using an AG Associates Heatpulse 410 rapid thermal annealing (RTA) system for times up to 120 s while anneals above 5 min were performed in a conventional furnace with a nitrogen ambient for times up to 360 min. The plan-view specimens were then chemically thinned from the backside. A JEOL 200 CX operating at 200 keV using a $\mathbf{g}_{220}$ two-beam imaging weak beam dark field condition was used to analyze the annealed samples. Defect evolution was then quantified from enlarged micrographs and defect and interstitial density counts were extracted.

III. RESULTS AND DISCUSSION

Figure 1 shows the defect density and trapped interstitial behavior for the 5, 10, and 30 keV energies following 750 °C anneals. The defects density decreases with time as expected for the three implant energies, but the defects that evolve for the 10 and 30 keV energies are different than that of the 5 keV energy. For the two higher energies, defect clusters grow into {311}'s with time, then dissolve, releasing trapped interstitials for dislocation loop growth. After 360 min of annealing, only large, stable dislocation loops are observed. For the lowest energy several different effects were observed: {311}'s were not observed for the 5 keV energy, and the small, unstable dislocation loops that did form completely dissolved before 60 min.

The interstitial behavior shown in Fig. 1(b) is stable up to 60 min, after which all energies exhibit a decrease in the

[a]Electronic mail: kingmse@aol.com

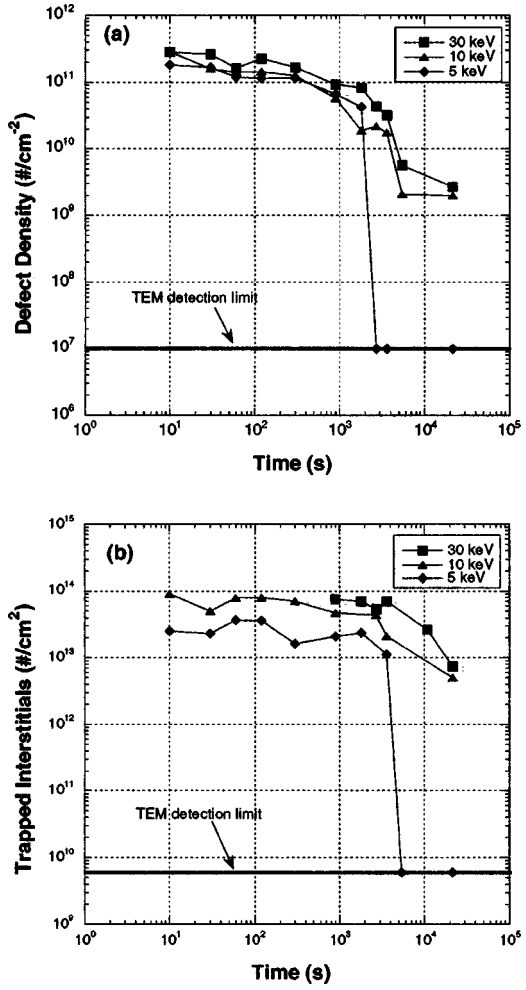

FIG. 1. Defect evolution of 30, 10, and 5 keV Ge^+ implants at 750 °C. After 45 min of annealing, complete defect dissolution occurs at the 5 keV energy as shown by (a) defect density and (b) trapped interstitials over time. The two higher energies form stable dislocation loops that are stable after 360 min anneals.

number of interstitials. The 5 keV energy shows the sharpest decrease and mirrors the defect evolution behavior shown in Fig. 1(a). It is evident from the defect evolution behavior shown in Fig. 1 that decreasing energy below 10 keV greatly affects the type of EOR defects formed and their stability upon annealing. A threshold for defect stability exists between the 5 and 10 keV implant energy levels.

To gain a further understanding into the 5 keV defect dissolution process, a surface lapping experiment was performed to determine the role of the free surface as an interstitial recombination sink. Previous studies of nonamorphizing Si^+ implants report that the surface acts as a recombination sink and influences defect evolution.[12–14] However, other studies of amorphizing implants show that EOR damage evolution is implant energy dependent and the surface proximity has no effect.[15,16] To isolate the surface proximity effect, the amorphous layer of a 10 keV specimen (thickness=180 Å) was mechanically lapped to less than that of the 5 keV amorphous layer thickness (thickness=100 Å) using colloidal silica, particle sizes of 0.2–0.6 μm, against rayon polishing pads. Ellipsometry was used for α-layer measurements during the lapping process while high-resolution TEM was used for the ultimate measurement.

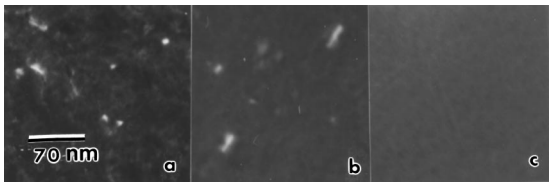

FIG. 3. Plan-view TEM micrographs for 60 min annealing times at 750 °C for (a) 10 keV, (b) 10 keV-lapped, and (c) 5 keV samples. Note that the 10 keV-lapped specimen follows the same defect evolution as the normal 10 keV energy.

Figure 2 shows high-resolution cross section TEM (XTEM) micrographs of the amorphous layer thickness for 10 keV-lapped, 10 keV, and 5 keV specimens. The measured amorphous layer thickness is 80, 180, and 100 Å, respectively. Reducing the amorphous layer thickness below that of the 5 keV energy isolates the surface effect variable during defect evolution. The 10 keV-lapped specimen was then annealed from 5–360 min at 750 °C. PTEM analysis shows that the defect evolution for the 10 keV-lapped specimen strongly resembles that of the 10 keV energy. Figure 3 shows PTEM micrographs of the 10 keV-lapped compared to 10 and 5 keV specimens after 60 min anneals. Qualitatively comparing defects, {311} dislocation unfaulting into loops as well as small dislocation loops are visible for the 10 keV-lapped and 10 keV specimens, while there are no defects present for the 5 keV specimen.

Figure 4 shows the defect density for the 10 keV-lapped specimen after annealing compared to those for the 5 and 10 keV energy. The 10 keV-lapped specimen does not exhibit dissolution of defects over the annealing schedule and dislocation loops remained after 360 min. This behavior shows that EOR damage is not greatly affected by free surface proximity even with amorphous layer thickness $<$100 Å and

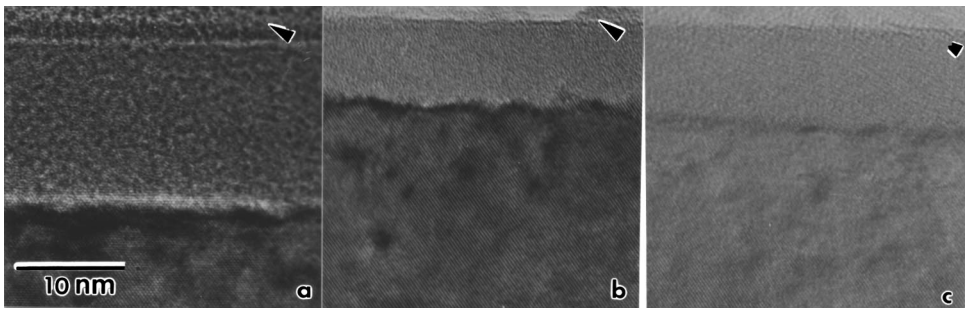

FIG. 2. High-resolution cross section NTEM micrographs of the amorphous layer thickness for (a) 10 keV, (b) 10 keV-lapped, and (c) 5 keV samples. 10 keV implants form an amorphous layer 180 Å thick. Arrows point to the surface layer. The 10 keV-lapped specimen's amorphous layer was reduced to 80 Å, less than the 100 Å 5 keV amorphous layer thickness.

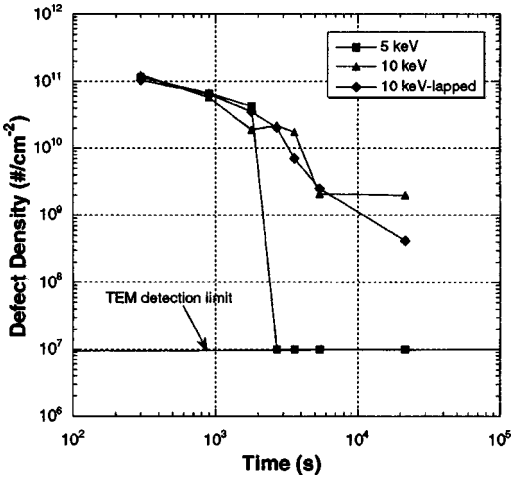

FIG. 4. Defect density evolution of the 10 keV-lapped samples annealed at 750 °C compared to the 10 and 5 keV energies. The 10 keV-lapper specimen follows the same trend as the 10 keV energy. This shows that EOR surface proximity is not the factor for the 5 keV defect dissolution.

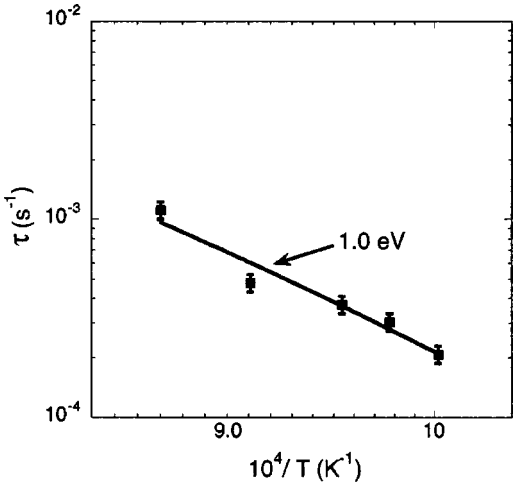

FIG. 6. Activation energy plot showing the defect dissolution times and temperatures. A best-fit exponential curve results in activation energy of 1.0 ± 0.1 eV.

that the observed defect dissolution in the 5 keV specimen is implant energy related.

To gain a further understanding of the defect dissolution process observed for the 5 keV energy implants, specimens were annealed at multiple temperatures to calculate the activation energy of the dissolution. Specimens were examined using PTEM in 5 min intervals near the dissolution window to identify when it occurred at temperatures of 725, 750, 775, 825, and 875 °C. The times and corresponding temperatures were plotted in an Arrhenius-type chart to calculate the activation energy.

Figure 5 shows defect densities from the five annealing times near the dissolution window. Dissolution times decrease as the annealing temperature increases as one would expect, but not to a large extent. The defect densities for the various temperatures show that the dissolution process occurs very rapidly upon its onset. Defect densities drop from the 10^9 range to undetectable levels within 5 min. This supports that the damage produced from low energy implants evolves into defects with a stability threshold, but the pathway for the dissolution is not known at this time.

Figure 6 is the dissolution times for the 5 keV energy and their corresponding temperatures modeled in Arrhenius form. The plot follows the behavior of the exponential $\tau = \tau_0 \exp\{-\Delta E/kT\}$, where $\tau_0 = 22.78\ \mathrm{s}^{-1}$ and $\Delta E = 1.0 \pm 0.1$ eV. Since the dissolution times were pinpointed within a 5 min range there is at least a 10% error in the times shown in Fig. 6. Previous studies of dislocation loop dissolution in silicon have always shown an activation energy of 4 to 5 eV.[17] The explanation for this has always been that Si self-diffusion was involved, which has an activation energy of $\sim$4.5 eV.[18,19] The activation energy for dislocation loop dissolution in the 5 keV implant is much lower than these prior values. It is unclear at this time why this is observed but further investigations into this phenomenon are in progress.

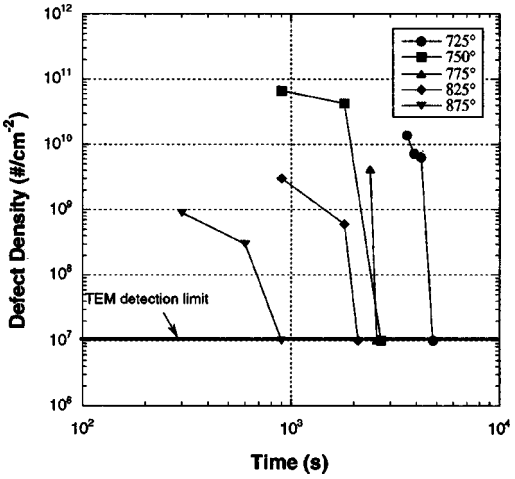

FIG. 5. Defect density over time for five temperatures near their dissolution times for the 5 keV energy at 750 °C. The dissolution process occurs rapidly, there is not a gradual decrease in defects over time as in higher energies.

IV. CONCLUSION

There is a defect stability threshold for Ge^+ amorphizing germanium implants with energy <10 keV. The defect evolution for the 5 keV energy does not involve formation of {311}'s that grow into dislocation loops like higher energies of 10 and 30 keV. The 5 keV energy forms small, unstable loops that rapidly dissolve within a small time window and do not form extended defects. Implantation energy is the dominant factor in the observed defect dissolution, the free surface does not play a significant role in this system. The dissolution activation energy was calculated to be 1.0 ± 0.1 eV. This low activation energy value suggests that at low implant energies, EOR damage forms unstable defects that use a different pathway from higher energies to evolve.

[1] E. Myers, G. A. Rozgonyi, D. K. Sadana, W. Maszara, J. J. Wortman, and J. Narayan, Mater. Res. Soc. Fall, Symp. B **52**, 107 (1985).
[2] M. C. Ozturk, J. J. Wortman, C. M. Osburn, A. Ajmera, G. A. Rozgonyi, E. Frey, W. K. Chu, and C. Lee, IEEE Trans. Electron Devices **35**, 659 (1988).
[3] S. N. Hong, G. A. Ruggles, J. J. Wortman, and M. C. Ozturk, IEEE Trans. Electron Devices **38**, 476 (1991).

[4] A. J. Murrel, E. J. Collart, and M. A. Foad, J. Vac. Sci. Technol. B **18**, 462 (2000).
[5] D. J. Eaglesham, P. A. Stolk, H. J. Gossman, and J. M. Poate, Appl. Phys. Lett. **65**, 2305 (1994).
[6] K. S. Jones, J. Liu, L. Zhang, V. Krishnamoorthy, and R. T. DeHoff, Nucl. Instrum. Methods Phys. Res. B **106**, 227 (1995).
[7] D. J. Eaglesham, A. Agarwal, T. E. Haynes, H. J. Gossmann, D. C. Jacobson, and J. M. Poate, Nucl. Instrum. Methods Phys. Res. B **120**, 1 (1996).
[8] A. Agarwal, T. E. Haynes, D. J. Eaglesham, H. J. Gossmann, D. C. Jacobson, J. M. Poate, and Y. E. Erokhin, Appl. Phys. Lett. **70**, 3332 (1997).
[9] J. Li and K. S. Jones, Appl. Phys. Lett. **73**, 3748 (1998).
[10] N. E. B. Cowern, G. Mannino, F. Roozeboom, P. A. Stolk, H. G. Gossmann, H. G. A. Huizing, J. G. M. van Berkum, N. N. Toan, and P. H. Woerlee, 195th ECS Meeting, Seattle, WA, 1999.
[11] M. A. Foad, A. J. Murrell, E. J. H. Collart, G. de Cock, D. Jennings, and M. I. Current, Mater. Res. Soc. Symp. Proc. **568**, 55 (1999).
[12] D. R. Lim, C. S. Rafferty, and F. P. Klemens, Appl. Phys. Lett. **67**, 2302 (1995).
[13] A. Agarwal, H.-J. Gossmann, D. J. Eaglesham, L. Pelaz, D. C. Jacobson, T. E. Haynes, and Y. E. Erokhin, Appl. Phys. Lett. **21**, 3141 (1997).
[14] C. D. Meekinson, C. Hill, C. D. Marsh, D. P. Gold, D. R. Boys, and G. R. Booker, Inst. Phys. Conf. Ser. **117**, 197 (1991).
[15] E. Ganin and A. Marwick, Mater. Res. Soc. **147**, 13 (1989).
[16] M. Omri, C. Bonafos, A. Claverie, A. Nejim, F. Cristano, D. Alquier, A. Martinez, and N. E. B. Cowern, Nucl. Instrum. Methods Phys. Res. B **120**, 5 (1996).
[17] T. E. Siedel, D. J. Lischner, C. S. Pai, R. V. Knoell, D. M. Maher, and D. C. Jacobson, Nucl. Instrum. Methods Phys. Res. B **7/8**, 251 (1985).
[18] F. J. Desmond, S. Kalbitzer, H. Mannsperger, and H. Damjantschitsch, Phys. Lett. **93A**, 503 (1983).
[19] W. Frank, U. Gosele, H. Mehrer, and A. Seger, *Diffusion in Crystalline Solids* (Academic, New York, 1984).